

Received:
20 October 2014Revised:
24 February 2015Accepted:
2 March 2015

doi: 10.1259/bjr.20140698

Cite this article as:
Park JM, Wu H-G, Kim JH, Carlson JNK, Kim K. The effect of MLC speed and acceleration on the plan delivery accuracy of VMAT. Br J Radiol 2015;88:20140698.

FULL PAPER

The effect of MLC speed and acceleration on the plan delivery accuracy of VMAT

**1,2,3,4 J M PARK, PhD, 1,2,3,5 H-G WU, MD, PhD, 1,2,3 J H KIM, MD, PhD, 6 J N K CARLSON, BS and
1 K KIM, MD, PhD**

¹Department of Radiation Oncology, Seoul National University Hospital, Seoul, Republic of Korea

²Institute of Radiation Medicine, Seoul National University Medical Research Center, Seoul, Republic of Korea

³Biomedical Research Institute, Seoul National University College of Medicine, Seoul, Republic of Korea

⁴Center for Convergence Research on Robotics, Advanced Institutes of Convergence Technology, Suwon, Republic of Korea

⁵Department of Radiation Oncology, Seoul National University College of Medicine, Seoul, Republic of Korea

⁶Program in Biomedical Radiation Sciences, Department of Transdisciplinary Studies, Seoul National University, Graduate School of Convergence Science and Technology, Seoul, Republic of Korea

Address correspondence to: Dr Kyubo Kim
E-mail: kyubokim@snu.ac.kr

Objective: To determine a new metric utilizing multileaf collimator (MLC) speeds and accelerations to predict plan delivery accuracy of volumetric modulated arc therapy (VMAT).

Methods: To verify VMAT delivery accuracy, gamma evaluations, analysis of mechanical parameter difference between plans and log files, and analysis of changes in dose-volumetric parameters between plans and plans reconstructed with log files were performed with 40 VMAT plans. The average proportion of leaf speeds ranging from 1 to $h\text{ cm s}^{-1}$ (S_{l-h} and $l-h = 0-0.4, 0.4-0.8, 0.8-1.2, 1.2-1.6$ and $1.6-2.0$), mean and standard deviation of MLC speeds were calculated for each VMAT plan. The same was carried out for accelerations in centimetre per second squared (A_{l-h} and $l-h = 0-4, 4-8, 8-12, 12-16$ and $16-20$). The correlations of those indicators to plan

delivery accuracy were analysed with Spearman's correlation coefficient (r_s).

Results: The $S_{1,2-1,6}$ and mean acceleration of MLCs showed generally higher correlations to plan delivery accuracy than did others. The highest r_s values were observed between $S_{1,2-1,6}$ and global 1%/2mm ($r_s = -0.698$ with $p < 0.001$) as well as mean acceleration and global 1%/2mm ($r_s = -0.650$ with $p < 0.001$). As the proportion of MLC speeds and accelerations >0.4 and 4 cm s^{-2} increased, the plan delivery accuracy of VMAT decreased.

Conclusion: The variations in MLC speeds and accelerations showed considerable correlations to VMAT delivery accuracy.

Advances in knowledge: As the MLC speeds and accelerations increased, VMAT delivery accuracy reduced.

Volumetric modulated arc therapy (VMAT) delivers a conformal prescription dose to the target volume while minimizing dose to normal tissues. This is accomplished by modulating photon beam intensities through the modulation of multileaf collimator (MLC) positions, gantry speeds and dose rates simultaneously at each control point (CP).¹⁻³ Although the modulation of photon beam intensity is a core feature of VMAT, excessive modulation of photon beam intensity increases uncertainty in the mechanical operation of the linear accelerator (linac) and also increases the number of small or irregular field shapes, resulting in differences in dose distributions between calculated and delivered plans.⁴ This can potentially cause not only poor tumour control but also damage to normal tissues. Therefore, pre-treatment quality assurance (QA) for each patient is routinely performed in the clinic for

verification that the plan is delivered as intended.^{3,5-9} Another method of verification to determine whether a VMAT plan is deliverable as intended or not is the analysis of dynamic log files registered in the linac control system during delivery.¹⁰⁻¹⁴ As a further method of analysis, it has been suggested that the dose distribution in patient CT images be reconstructed with those dynamic log files and compared with that of the original treatment plan.¹⁵

On the other hand, several studies have suggested modulation indices for VMAT, which can quantify and evaluate the degree of modulation at the planning stage to verify the plan delivery accuracy.^{4,16-24} Modulation indices have an advantage compared with pre-treatment QA or dynamic log file analysis in that clinical resources required to

evaluate the degree of modulation of VMAT plans are spared. Masi et al¹⁸ suggested the modulation complexity score (MCS) for VMAT (MCS_v) as well as the leaf travel MCS (LTMCS) as modulation indices for VMAT, both of which focus on the MLC movement and the aperture shapes defined by MLCs. Li and Xing¹⁷ suggested a modulation index for VMAT (MI_{SPORT}) by combining the segmental monitor unit (MU) and variations in MLC positions. We also suggested a modulation index adopting previously suggested methodology by Webb²⁴ by quantifying MLC speeds, MLC accelerations, gantry rotation accelerations and dose-rate variations at each CP simultaneously.²⁵

In terms of the mechanical operation of linacs for VMAT, Nicolini et al²⁶ showed the reliability of variations in gantry rotational speed in relation to dose-rate variations for VMAT. In the previous study, we demonstrated that the effect of MLC movements on VMAT delivery accuracy was larger than that of gantry angle rotation or dose-rate variation.²⁵ It has been demonstrated that the modulation of MLC movement is a critical factor influencing plan delivery accuracy of VMAT.^{9,18,25,26} Although considerable influence of MLC movement on plan delivery accuracy of VMAT is recognized, a more detailed relationship of VMAT plan delivery accuracy to the patterns of MLC movement, that is, variations in MLC speed and acceleration, is unclear. Thus, we investigated the effect of variations in MLC speeds and accelerations on plan delivery accuracy in this study. Furthermore, we tried to predict the plan delivery accuracy of VMAT with specific MLC speed and acceleration information.

The speeds of each MLC between each CP were calculated with clinically acceptable VMAT plans and divided into several groups according to the magnitude of MLC speed. The same was carried out for MLC acceleration. After that, the ratios of the CP numbers in a group to the total number of CPs were calculated. The correlations of those calculated values to the plan delivery accuracy were analysed using the Spearman's rank correlation coefficient (r_s). The plan delivery accuracy was evaluated using two-dimensional (2D) global and local gamma-index methods with various gamma criteria. The global gamma index calculates the difference in dose relative to a specific dose, such as the maximum dose, while the local gamma index calculates dose difference relative to the current measurement point.²⁷ Dynamic log file analysis and changes in dose–volumetric parameters between the original treatment plans and plans reconstructed with log files were also investigated. Through evaluation of the correlations of each group to plan delivery accuracy, the effects of variations in MLC speeds and accelerations on VMAT plan delivery accuracy were investigated.

METHODS AND MATERIALS

Volumetric modulated arc therapy planning

The VMAT plans analysed in our previous study were also used in this study.²⁵ Randomly, 20 head and neck (H&N) and 20 prostate VMAT plans were retrospectively selected from plans previously used for patient treatment in the Department of Radiation Oncology, Seoul National University Hospital. For the generation of both prostate and H&N VMAT plans, 6-MV photon beams of Trilogy® with Millennium™ 120 MLC (Varian® Medical Systems, Palo Alto, CA) were used. All VMAT

plans were generated using two full arcs with the Eclipse system (Varian Medical Systems). The progressive resolution optimizer 3 (PRO3, v. 10; Varian Medical Systems) was used for optimization. For the calculation of dose distributions, the Anisotropic Analytic Algorithm v. 10 (Varian Medical Systems) was used with a calculation grid of 2.5 mm. For the patients with prostate cancer in our institution, a primary plan delivering 50.4 Gy (daily, 1.8 Gy) to the primary target volume and a boost plan delivering 30.6 Gy (daily, 1.8 Gy) to the boost target volume were generated. Only primary plans were analysed in this study. A primary target volume was defined with a margin of 2 cm from the prostate and seminal vesicles in all directions except the inferior and posterior directions. To reduce dose to the rectal wall, a margin of 1 cm was added to the inferior and posterior directions. In the case of H&N VMAT plans, the simultaneous integrated boost technique was used with a total of three target volumes. A margin of 0.3 cm was added in all directions from the clinical target volume. Prescription doses of 67.5 Gy (daily, 2.25 Gy), 54 Gy (daily, 1.8 Gy) and 48 Gy (daily, 1.6 Gy) were delivered to Targets 1, 2 and 3, respectively.

Verification of volumetric modulated arc therapy plan delivery accuracy

A total of three types of verification methods used in our previous study²⁵ were adopted to evaluate the VMAT delivery accuracy in this study.

Gamma-index method with MapCHECK2™ detector array

2D dose distributions of each VMAT plan were measured with a MapCHECK2 detector array (Sun Nuclear Corporation, Melbourne, FL). When measuring 2D dose distributions, the MapCHECK2 detector array was inserted into a MapPHAN™ (Sun Nuclear Corporation), which is a solid water phantom with a hole for insertion of the MapCHECK2 detector array. For comparison, the reference planar dose distributions of each VMAT plan were calculated in a virtual water phantom with a calculation grid of 1 mm, which is the finest resolution of the Eclipse system. The mass density of that virtual water phantom in the Eclipse system was manually modified and assigned to match the calculated and measured values with the MapCHECK2 detector array inserted into MapPHAN, in accordance with manufacturer recommendations. Before the measurement of 2D dose distributions for gamma evaluations, the output of the linac was calibrated with a measured value based on the American Association of Physicists in Medicine Task Group 51 protocol.²⁸ After that, the absolute reading of the MapCHECK2 detector array was calibrated following the manufacturer provided protocol. The relative readings of each detector in the MapCHECK2 detector array were also calibrated according to the protocol provided by the manufacturer. After measurements of the VMAT plan dose distributions, both global and local gamma evaluations were performed with SNC patient software v. 6.1.2 (Sun Nuclear Corporation). Gamma criteria of 2%/2, 1%/2 and 2%/1 mm were used for gamma evaluation. As recommended by previous studies for pre-treatment QA for VMAT, gamma criteria of 3%/3 and 1%/1 mm were not used in this study.^{7,8,29} Any values that were <10% of the maximum dose were not evaluated when performing gamma evaluations as often cited in the literature.^{8,30,31}

Analysis of log files generated during volumetric modulated arc therapy delivery

During the acquisition of planar dose distributions with the MapCHECK2 detector array, dynamic log files, which are records of actual gantry angles and delivered MUs at each CP of a VMAT plan, were acquired. Simultaneously, DynaLog files (Varian Medical Systems), which are a record of MLC positions every 50 ms, were acquired for each VMAT plan. These two types of log files were combined using an in-house program written in MATLAB® v. 8.1 (MathWorks®, Natick, MA) to generate digital imaging and communications in medicine-radiotherapy (DICOM-RT)-formatted VMAT plan files. For each VMAT plan, the differences in MLC positions, gantry angles and delivered MUs at each CP between the original treatment plan and the DICOM-RT-formatted VMAT plan were calculated.

Analysis of dose-volumetric parameters

The DICOM-RT-formatted VMAT plans were imported into the Eclipse system, and dose distributions in patient CT image sets identical to those used for treatment planning were calculated for each VMAT plan. The DICOM-RT-formatted VMAT plans included information of every MLC position, gantry angles and MUs at each CP. Using the PRO3 algorithm, each plan had a total of 178 CPs per full arc, thus the CP intervals were 2.0341°. Just as in original VMAT plans generated in the Eclipse system, the DICOM-RT-formatted plans used discrete information from each CP to calculate the dose distributions in the CT image set of a patient. Calculation grids of 2.5 mm, identical to the original treatment plans, were used for dose calculation. After calculation of dose distributions, clinically significant dose–volumetric parameters were calculated with identical structure sets as those used for treatment planning. For the target volume, the dose received by 95% of the target volume ($D_{95\%}$), $D_{5\%}$, minimum, maximum and mean dose to the target volume were calculated. For prostate organs at risk (OARs), $D_{20\%}$ of rectal wall and bladder, mean dose to the rectal wall, bladder and femoral head, and $D_{50\%}$ of femoral head were calculated. For H&N OARs, mean dose to each parotid gland and the maximum dose to the spinal cord, the brain stem, each lens, optic chiasm and each optic nerve were calculated. The differences in dose–volumetric parameters between original treatment plans and the DICOM-RT-formatted plans were calculated.

Analysis on the MLC speeds and accelerations of VMAT plans

CPs in VMAT plans (RapidArc®; Varian Medical Systems) are defined in gantry rotation intervals of 2.0341°, therefore adjacent CPs do not necessarily have equal time intervals, thus the time between CPs must be calculated in advance to allow determination of MLC speeds and accelerations. According to manufacturer specifications, the maximum gantry speed and the maximum dose rate were 4.8° s⁻¹ and 600 MU min⁻¹ (*i.e.* 10 MU s⁻¹), respectively, thus we calculated time between each CP based on this information. The maximum MU able to be delivered without slowing down the gantry rotation is $(2.0341 \times 10 \text{ MU s}^{-1}) / (4.8^\circ \text{ s}^{-1}) = 4.238 \text{ MU}$. If it is necessary to deliver MU >4.238 MU, the gantry rotation speed should be

decreased. In this case, the dose rate is maintained at the maximum of 600 MU min⁻¹. Therefore, (1) if the value of MU is ≤4.238 MU at a given CP, the time between CP is $2.0341^\circ / (4.8^\circ \text{ s}^{-1}) = 0.424 \text{ s}$, while (2) if the value of MU is >4.238 MU, the time is $(\text{the MU at that CP}) / (10 \text{ MU s}^{-1})$. With this time information, the speed of each leaf (Leaf speed_{*i*}) at each CP was calculated as follows.

$$\text{Leaf speed}_i = \frac{|\text{Leaf}_i - \text{Leaf}_{i+1}|}{\text{Time}_i} \quad (1)$$

where Leaf_{*i*} is the position of the leaf at the *i*th CP, and Time_{*i*} is the time between the *i*th CP and the (*i*+1)th CP.

For each leaf, the number of CPs with Leaf speeds ranging from *l* to *h* cm s⁻¹ were counted and divided by the total number of CPs for each VMAT plan (S_{l-h}). Since no Leaf speed_{*i*} > 2 cm s⁻¹ was observed in VMAT plans analysed in this study, the combinations of *l* and *h* in this study were from 0 to 0.4 cm s⁻¹ ($S_{0-0.4}$), from 0.4 to 0.8 cm s⁻¹ ($S_{0.4-0.8}$), from 0.8 to 1.2 cm s⁻¹ ($S_{0.8-1.2}$), from 1.2 to 1.6 cm s⁻¹ ($S_{1.2-1.6}$) and from 1.6 to 2.0 cm s⁻¹ ($S_{1.6-2.0}$). After that, the average value of S_{l-h} of every MLC for each section was calculated for each VMAT plan.

To take acceleration into account, the acceleration of each leaf (Leaf accel_{*i*}) at each CP was calculated as follows.

$$\text{Leaf accel}_i = \frac{|\text{Leaf speed}_i - \text{Leaf speed}_{i+1}|}{\text{Time}_{i+1}} \quad (2)$$

For each leaf, the number of CPs with leaf accelerations ranging from *l* to *h* cm s⁻² were counted and divided by the total number of CPs for each VMAT plan (A_{l-h}). Since no Leaf accel_{*i*} > 20 cm s⁻² was observed in VMAT plans analysed in this study, the combinations of *l* and *h* in this study were from 0 to 4 cm s⁻² (A_{0-4}), from 4 to 8 cm s⁻² (A_{4-8}), from 8 to 12 cm s⁻² (A_{8-12}), from 12 to 16 cm s⁻² (A_{12-16}) and from 16 to 20 cm s⁻² (A_{16-20}). After that, average values of A_{l-h} of every MLC for each section were calculated for each VMAT plan.

For each VMAT plan, mean values and standard deviations (SDs) of every Leaf speed_{*i*} in centimetre per second unit and Leaf accel_{*i*} in centimetre per second square unit were also calculated.

Correlation analysis

To investigate the effect of MLC speed and acceleration on the VMAT plan delivery accuracy, correlations of S_{l-h} , A_{l-h} , mean values and SDs of Leaf speed_{*i*} and Leaf accel_{*i*} to the plan delivery accuracy were analysed with Spearman's rank correlation coefficient (r_s). To examine the statistical significance of the values of r_s , *p*-values were acquired using a two-tailed unpaired parameter condition. Since the data in this study represented a relatively small sample size, and did not consider missing values, *p*-values were computed with the exact permutation distributions. Plan delivery accuracy in this study was characterized using three separate methods as mentioned above.²⁵ The first method was to use both global and local gamma passing rates with 2%/2, 1%/2 and 2%/1 mm. The second

method was to investigate mechanical parameter differences such as MLC positional differences, gantry angle differences and MU differences at each CP between original treatment plans and DICOM-RT files generated with the log files. Finally, dose-volumetric parameter differences between the original plans and DICOM-RT reconstructed VMAT plan files. For the correlation tests of both gamma passing rates and mechanical parameter differences, a total of 40 VMAT plans were used, including both prostate and H&N VMAT plans, while a total of 20 VMAT plans were used to test the correlations with dose-volumetric differences as the OARs of the prostate plans were different from those of the H&N plans.

RESULTS

The values of S_{l-h} , A_{l-h} and mean values of Leaf speed_i and Leaf accel_i

The values of S_{l-h} , A_{l-h} and mean values of Leaf speed_i and Leaf accel_i are shown in Table 1. As mentioned above, no values of Leaf speed_i and Leaf accel_i > 2 and 20 cm s⁻², respectively, were observed. Therefore, the summed value of S_{l-h} of every section in a VMAT plan was always 1. The same applied for A_{l-h} . To illustrate the differences in the patterns of MLC speed variations according to the plan delivery accuracy, examples of the two plans showing the highest delivery accuracy (prostate VMAT 1 and 2) and the two showing the worst delivery accuracy (H&N VMAT 1 and 2) are shown in Figure 1. Highly modulated VMAT plans contained larger proportions of CPs with high MLC speeds than did lowly modulated VMAT plans. For MLC accelerations, representative examples of the two VMAT plans that showed the highest plan delivery accuracy (prostate VMAT 1 and 2), as well as those of the two VMAT plans that showed the worst plan delivery accuracy (H&N VMAT 1 and 2) are shown in Figure 2. Highly modulated VMAT plans contained larger proportions of CPs with MLC accelerations > 4 cm s⁻² than did lowly modulated VMAT plans. The values of S_{l-h} calculated with prostate VMAT plans were always different from

those calculated with H&N VMAT plans with statistical significance, as displayed in Table 1 ($p < 0.001$). With the exception of $S_{0-0.4}$, the values of S_{l-h} of H&N VMAT plans were always higher than those of prostate VMAT plans. The mean value of MLC speeds of H&N VMAT plans was higher than that of prostate VMAT plans ($p < 0.001$). All values of A_{l-h} of H&N VMAT plans, except A_{0-4} , were equal to or higher than those of prostate VMAT plans with statistical significances ($p < 0.001$). The mean value of MLC acceleration of H&N VMAT plans was higher than that of prostate VMAT plans ($p < 0.001$).

Gamma passing rates vs variations in multileaf collimator movements

Gamma passing rates vs variations in multileaf collimator speed

The values of r_s and corresponding p -values for S_{l-h} , mean values and SDs of MLC speeds to both global and local gamma passing rates are shown in Table 2.

The r_s values of S_{l-h} as well as mean values and SDs of MLC speeds to global gamma passing rates with 2%/2 and 1%/2 mm were always statistically significant showing p -values < 0.008. In the cases of local gamma passing rates, all values of r_s were statistically significant to gamma passing rates with every gamma criterion ($p < 0.02$). For both global and local gamma passing rates, the r_s values of $S_{0-0.4}$ always had positive signs, while those of the other S_{l-h} always had negative signs. Therefore, as the values of $S_{0-0.4}$ increased, the values of both global and local gamma passing rates increased. However, as the proportion of CPs with MLC speeds > 0.4 cm s⁻¹ increased, the values of both global and local gamma passing rates decreased. As mean values and SDs of MLC speeds increased, both global and local gamma passing rates decreased. The highest r_s value was observed between $S_{1.2-1.6}$ and global gamma passing rates with 1%/2 mm ($r_s = -0.698$ with $p < 0.001$).

Table 1. The average proportion of control point (CP) numbers belonging to particular sections according to the magnitude of multileaf collimator (MLC) speed and acceleration and average values of mean MLC speed and acceleration

Plan type	MLC speed					
	$S_{0-0.4}$	$S_{0.4-0.8}$	$S_{0.8-1.2}$	$S_{1.2-1.6}$	$S_{1.6-2.0}$	Mean speed
Prostate VMAT	0.637 ± 0.026	0.139 ± 0.011	0.050 ± 0.006	0.028 ± 0.003	0.147 ± 0.014	0.476 ± 0.672
H&N VMAT	0.434 ± 0.033	0.181 ± 0.011	0.082 ± 0.007	0.050 ± 0.007	0.253 ± 0.025	0.772 ± 0.745
<i>p</i> -value	<0.001	<0.001	<0.001	<0.001	<0.001	<0.001
Plan type	MLC acceleration					
	A_{0-4}	A_{4-8}	A_{8-12}	A_{12-16}	A_{16-20}	Mean acceleration
Prostate VMAT	0.903 ± 0.016	0.080 ± 0.013	0.017 ± 0.004	0.000 ± 0.000	0.000 ± 0.000	1.311 ± 1.849
H&N VMAT	0.853 ± 0.015	0.123 ± 0.011	0.025 ± 0.004	0.000 ± 0.000	0.000 ± 0.000	1.825 ± 2.075
<i>p</i> -value	<0.001	<0.001	<0.001	0.416	0.932	<0.001

A_{l-h} , the proportion of number of CPs of MLC accelerations ranging from / to h cm s⁻²; H&N, head and neck; *p*-value, *p*-values showing statistical significances of differences between S_{l-h} (A_{l-h}) of prostate plans and S_{l-h} (A_{l-h}) of H&N plans; S_{l-h} , the proportion of number of CPs with MLC speeds ranging from / to h cm s⁻²; VMAT, volumetric modulated arc therapy.

Gamma passing rates vs variations in multileaf collimator accelerations

The values of r_s and corresponding p -values for A_{L-h} , mean values and SDs of MLC accelerations to both global and local gamma passing rates are shown in Table 3.

With the exception of A_{12-16} and A_{16-20} , the r_s values of A_{L-h} as well as mean and SDs of MLC accelerations to global gamma passing rates with 2%/2 and 1%/2 mm were always statistically significant ($p < 0.03$). In the cases of local gamma passing rates, all r_s values were statistically significant except r_s between A_{12-16} and passing rates with 1%/2 mm and A_{16-20} and passing rates with 2%/2 and 1%/2 mm. The r_s values of A_{0-4} always had positive signs, while those of the other A_{L-h} always had negative signs to both global and local gamma passing rates, showing the same tendency as S_{L-h} . The highest r_s values were observed between mean acceleration of MLC and passing rates with global 1%/2 mm ($r_s = -0.650$ with $p < 0.001$).

Differences in mechanical parameters between original plans and log files vs variations in MLC movements

Differences in mechanical parameters between original plans and log files vs variations in MLC speeds

The values of r_s and corresponding p -values of S_{L-h} , mean values and SDs of MLC speeds to the differences in mechanical parameters between plan and delivery are shown in Table 4. All r_s values of S_{L-h} , mean speed and SD of MLC to the MLC

positional errors and gantry angle errors were statistically significant, always showing $p < 0.001$. No statistically significant correlation of those indicators to MU errors was observed ($p > 0.05$). The r_s value between $S_{0-0.4}$ and MLC errors showed a negative correlation, while the r_s values between the other S_{L-h} and MLC errors showed positive correlations. This tendency was opposite in gantry angle errors. Therefore, as the proportion of CPs with MLC speeds $<0.4 \text{ cm s}^{-1}$ increased, the MLC error decreased but gantry angle error increased. On the other hand, as the proportion of CPs with MLC speeds $>0.4 \text{ cm s}^{-1}$ increased, the MLC error increased but gantry angle error decreased. For MLC errors, the highest r_s value was observed with $S_{0-0.4}$ ($r_s = -0.927$ with $p < 0.001$). For gantry angle errors, the highest correlation was observed at $S_{1.2-1.6}$ ($r_s = -0.694$ with $p < 0.001$).

Differences in mechanical parameters between original plans and log files vs variations in MLC accelerations

The values of r_s and corresponding p -values of A_{L-h} , mean values and SDs of MLC accelerations to the differences in mechanical parameters between the original treatment plan and log files recorded during delivery are shown in Table 4. All r_s values of A_{L-h} , mean MLC accelerations and SDs of MLC accelerations to the MLC positional errors and gantry angle errors were statistically significant ($p < 0.001$) except A_{12-16} and A_{16-20} . Similar to the results of MLC speed, no statistically significant correlation to MU errors was observed ($p > 0.05$). The r_s value between A_{0-4} and MLC errors showed a negative correlation, while the r_s

Figure 1. The number of control points in a volumetric modulated arc therapy (VMAT) plan are plotted according to the speeds of multileaf collimator (MLC). VMAT plans for prostate cancer, which showed superior plan delivery accuracy (a, b), as well as VMAT plans for head and neck cancer, which showed inferior plan delivery accuracy (c, d), are shown.

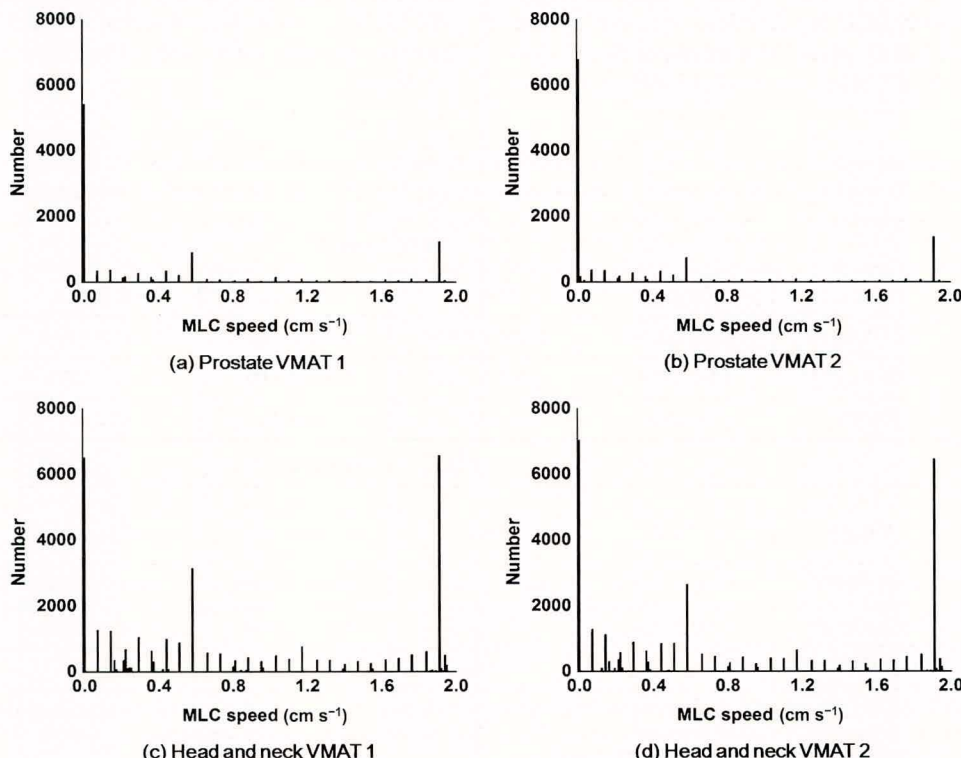
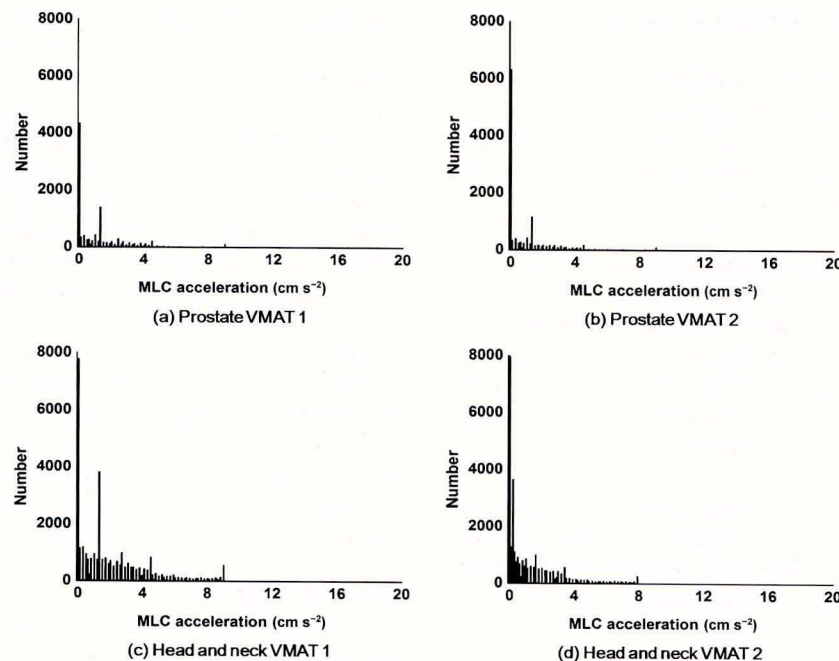


Figure 2. The number of control points in a volumetric modulated arc therapy (VMAT) plan are plotted according to the accelerations of multileaf collimator (MLC). Volumetric modulated arc therapy plans for prostate cancer, which showed superior plan delivery accuracy (a, b) as well as VMAT plans for head and neck cancer, which showed inferior plan delivery accuracy (c, d) are shown.



values between the other A_{l-h} and MLC errors showed positive correlations. Just as in the results of the MLC speed analysis, this tendency was opposite for gantry angle errors. For both MLC

errors and gantry angle errors, the highest r_s values were observed with A_{4-8} ($r_s = 0.843$ with $p < 0.001$ and $r_s = -0.677$ with $p < 0.001$, respectively).

Table 2. Spearman's rank correlation coefficients between gamma passing rates and S_{l-h}

Metric	2%/2 mm		1%/2 mm		2%/1 mm	
	r_s	p -value	r_s	p -value	r_s	p -value
Global gamma passing rates						
$S_{0-0.4}$	0.479	0.002	0.674	<0.001	0.301	0.059
$S_{0.4-0.8}$	-0.458	0.003	-0.644	<0.001	-0.258	0.108
$S_{0.8-1.2}$	-0.511	0.001	-0.690	<0.001	-0.338	0.033
$S_{1.2-1.6}$	-0.489	0.001	-0.698	<0.001	-0.319	0.045
$S_{1.6-2.0}$	-0.471	0.002	-0.662	<0.001	-0.283	0.076
Mean speed	-0.470	0.002	-0.674	<0.001	-0.283	0.077
SD speed	-0.417	0.007	-0.611	<0.001	-0.220	0.172
Local gamma passing rates						
$S_{0-0.4}$	0.540	<0.001	0.584	<0.001	0.522	0.001
$S_{0.4-0.8}$	-0.489	0.001	-0.554	<0.001	-0.404	0.010
$S_{0.8-1.2}$	-0.526	<0.001	-0.559	<0.001	-0.512	0.001
$S_{1.2-1.6}$	-0.508	0.001	-0.546	<0.001	-0.489	0.001
$S_{1.6-2.0}$	-0.498	0.001	-0.553	<0.001	-0.491	0.001
Mean speed	-0.536	<0.001	-0.579	<0.001	-0.515	0.001
SD speed	-0.420	0.007	-0.475	0.002	-0.413	0.008

r_s , Spearman's rho; SD, standard deviation; S_{l-h} , the proportion of number of control points with multileaf collimator speeds ranging from l to $h \text{ cm s}^{-2}$.

Differences in dose–volumetric parameters between the original treatment plan and plans reconstructed with log files vs variations in MLC movements

Volumetric modulated arc therapy plans for prostate cancer

The statistically significant r_s values and corresponding p -values of the S_{l-h} , A_{l-h} , mean values and SDs of MLC speed and accelerations to the differences in dose–volumetric parameters between original treatment plans and plans reconstructed with log files for prostate cancer are shown in Table 5.

In the case of MLC speed, $S_{0.4-0.8}$ showed statistically significant correlations to the changes in dose–volumetric parameters most frequently (four cases). The highest correlation was observed between $S_{1.2-1.6}$ and $D_{95\%}$ of target volume ($r_s = 0.563$ with $p = 0.01$). The r_s values of $S_{0-0.4}$ had negative signs and the other S_{l-h} had positive signs, just as in the results of gamma passing rates and mechanical parameter differences.

For MLC acceleration, A_{16-20} showed statistically significant correlations to the changes in dose–volumetric parameters most frequently (three cases). The highest correlation was observed between A_{16-20} and mean dose to target volume ($r_s = 0.473$ with $p = 0.035$).

Volumetric modulated arc therapy plans for head and neck cancer

The statistically significant values of r_s and corresponding p -values of the S_{l-h} , A_{l-h} , mean values and SDs to MLC speed and

accelerations to the differences in dose–volumetric parameters between original treatment plans and the plans reconstructed with log files for H&N cancer are shown in Table 6. For both MLC speeds and accelerations, statistically significant r_s values were observed more frequently in H&N VMAT plans than in prostate VMAT plans.

In the case of MLC speed, $S_{0.8-1.2}$ and $S_{1.2-1.6}$ showed statistically significant correlations to the changes in dose–volumetric parameters most frequently (both 11 cases). The highest correlation was observed between $S_{1.2-1.6}$ and the maximum dose to Target 3 ($r_s = 0.747$ with $p < 0.001$). The r_s values of $S_{0-0.4}$ and $S_{0.4-0.8}$ had negative signs, while the other S_{l-h} had positive signs.

In the case of MLC acceleration, mean acceleration showed statistically significant correlations to the dose–volumetric parameters most frequently (11 cases). The highest correlation was observed between mean acceleration and the minimum dose to Target 3 ($r_s = 0.694$ with $p = 0.001$). The r_s values of A_{0-4} had negative sign, and the other A_{l-h} had positive signs, showing the identical tendency as the other results.

DISCUSSION

As demonstrated by Kerns et al,³² restricting the maximum MLC speed can improve VMAT delivery accuracy. In this study, by correlation analysis, we demonstrated that not only MLC speeds but also MLC accelerations could affect the VMAT delivery accuracy. Both mean MLC speed and acceleration showed considerable correlations to the results acquired from various

Table 3. Spearman's rank correlation coefficients between gamma passing rates and A_{l-h}

Metric	2%/2 mm		1%/2 mm		2%/1 mm	
	r_s	p -value	r_s	p -value	r_s	p -value
Global gamma passing rates						
A_{0-4}	0.477	0.002	0.643	<0.001	0.267	0.096
A_{4-8}	-0.468	0.002	-0.644	<0.001	-0.264	0.100
A_{8-12}	-0.350	0.027	-0.473	0.002	-0.182	0.261
A_{12-16}	-0.226	0.161	-0.293	0.066	-0.197	0.223
A_{16-20}	-0.225	0.163	-0.253	0.116	-0.323	0.042
Mean accel.	-0.476	0.002	-0.650	<0.001	-0.253	0.115
SD accel.	-0.407	0.009	-0.575	<0.001	-0.228	0.158
Local gamma passing rates						
A_{0-4}	0.468	0.002	0.510	0.001	0.456	0.003
A_{4-8}	-0.465	0.003	-0.505	0.001	-0.447	0.004
A_{8-12}	-0.368	0.019	-0.370	0.019	-0.378	0.016
A_{12-16}	-0.362	0.022	-0.289	0.070	-0.426	0.006
A_{16-20}	-0.224	0.166	-0.272	0.089	-0.372	0.018
Mean accel.	-0.516	0.001	-0.543	<0.001	-0.479	0.002
SD accel.	-0.447	0.004	-0.454	0.003	-0.455	0.003

accel., acceleration; A_{l-h} , the proportion of number of control points of multileaf collimator accelerations ranging from l to $h \text{ cm s}^{-2}$; r_s , Spearman's rho; SD, standard deviation.

Table 4. Spearman's rank correlation coefficients between mechanical parameter differences at each control point (CP) and S_{l-h} as well as A_{l-h}

Metric	MLC position		Gantry angle		MU	
	r_s	p-value	r_s	p-value	r_s	p-value
$S_{0-0.4}$	-0.927	<0.001	0.615	<0.001	0.096	0.557
$S_{0.4-0.8}$	0.760	<0.001	-0.531	<0.001	-0.057	0.726
$S_{0.8-1.2}$	0.878	<0.001	-0.675	<0.001	-0.119	0.466
$S_{1.2-1.6}$	0.869	<0.001	-0.694	<0.001	-0.195	0.229
$S_{1.6-2.0}$	0.902	<0.001	-0.626	<0.001	-0.138	0.397
Mean speed	0.915	<0.001	-0.621	<0.001	-0.126	0.437
SD speed	0.857	<0.001	-0.622	<0.001	-0.095	0.562
<hr/>						
A_{0-4}	-0.835	<0.001	0.669	<0.001	0.196	0.225
A_{4-8}	0.843	<0.001	-0.677	<0.001	-0.184	0.256
A_{8-12}	0.688	<0.001	-0.564	<0.001	-0.131	0.421
A_{12-16}	0.202	0.211	-0.034	0.834	-0.110	0.501
A_{16-20}	0.255	0.112	-0.177	0.276	0.085	0.602
Mean accel.	0.840	<0.001	-0.659	<0.001	-0.172	0.288
SD accel.	0.799	<0.001	-0.631	<0.001	-0.118	0.467

accel., acceleration; A_{l-h} , the proportion of number of CPs of MLC accelerations ranging from l to $h \text{ cm s}^{-2}$; MLC, multileaf collimator; MU, monitor unit; r_s , Spearman's rho; SD, standard deviation; S_{l-h} , the proportion of number of CPs with MLC speeds ranging from l to $h \text{ cm s}^{-2}$.

VMAT verification methods. As the MLC speed and MLC acceleration increased, VMAT delivery accuracy decreased. This result is consistent with results demonstrated in our previous

study.²⁵ As a detailed analysis, the r_s values of S_{l-h} and A_{l-h} to VMAT delivery accuracy indicated that the VMAT delivery accuracy became worse if the proportions of MLC speeds

Table 5. Statistically significant Spearman's rank correlation coefficients of the differences in dose-volumetric parameters between treatment plan and delivery to S_{l-h} and A_{l-h} of prostate volumetric modulated arc therapy plans

Dose-volumetric parameter	$S_{0-0.4}$	$S_{0.4-0.8}$	$S_{1.2-1.6}$	$S_{1.6-2.0}$	Mean speed	Standard deviation speed	A_{4-8}	A_{16-20}	Mean accel.
Target volume									
$D_{95\%}$	r_s	-	0.529	0.563	-	0.512	-	0.460	0.464
	p-value	-	0.017	0.010	-	0.021	-	0.041	0.040
$D_{5\%}$	r_s	-	0.533	-	-	-	-	-	-
	p-value	-	0.016	-	-	-	-	-	-
Maximum dose	r_s	-	-	0.490	-	-	-	-	-
	p-value	-	-	0.028	-	-	-	-	-
Mean dose	r_s	-	0.548	-	-	-	-	0.473	-
	p-value	-	0.012	-	-	-	-	0.035	-
Organs at risk									
Rectal wall $D_{20\%}$	r_s	-0.452	0.472	0.527	0.507	0.534	0.501	0.461	-
	p-value	0.046	0.036	0.017	0.023	0.015	0.024	0.041	-
Femoral head mean dose	r_s	-	-	-	-	-	-	-	0.449
	p-value	-	-	-	-	-	-	-	0.047

accel., acceleration; A_{l-h} , the proportion of number of CPs of MLC accelerations ranging from l to $h \text{ cm s}^{-2}$; CP, control point; $D_{n\%}$, dose received by $n\%$ of volume of structure; r_s , Spearman's rho; S_{l-h} , the proportion of number of CPs with MLC speeds ranging from l to $h \text{ cm s}^{-2}$.

Table 6. Statistically significant Spearman's rank correlation coefficients of the differences in dose-volumetric parameters between treatment plan and delivery to S_{i-h} and A_{i-h} of head and neck volumetric modulated arc therapy plans

Dose-volumetric parameter	$S_{0-0.4}$	$S_{0.4-0.8}$	$S_{0.8-1.2}$	$S_{1.2-1.6}$	$S_{1.6-2.0}$	Mean speed	A_{0-4}	A_{4-8}	A_{16-20}	Mean acceleration
Target 1										
$D_{95\%}$	r_s	—	—	0.677	0.464	—	—	—	—	0.464
	p-value	—	—	0.001	0.039	—	—	—	—	0.039
$D_{5\%}$	r_s	—	—	0.648	0.541	—	—	—	—	0.462
	p-value	—	—	0.002	0.014	—	—	—	—	0.040
Mean	r_s	—	—	0.675	0.616	—	—	—	—	0.495
	p-value	—	—	0.001	0.004	—	—	—	—	0.026
Target 2										
$D_{95\%}$	r_s	—	—	0.467	0.451	—	—	—	—	0.480
	p-value	—	—	0.038	0.046	—	—	—	—	0.032
$D_{5\%}$	r_s	—	—	0.702	0.552	—	—0.529	0.531	—	0.675
	p-value	—	—	0.001	0.013	—	0.018	0.017	—	0.001
Mean	r_s	—	—	0.647	0.670	—	-0.461	0.465	—	0.623
	p-value	—	—	0.002	0.001	—	0.041	0.039	—	0.003
Target 3										
$D_{95\%}$	r_s	—	—	0.519	0.515	—	—	—	—	0.563
	p-value	—	—	0.023	0.024	—	—	—	—	0.012
$D_{5\%}$	r_s	—	—	0.674	0.597	—	-0.476	0.473	—	0.552
	p-value	—	—	0.002	0.007	—	0.039	0.041	—	0.014
Min.	r_s	-0.569	—	0.651	0.579	0.628	0.586	-0.577	0.630	—0.694
	p-value	0.011	—	0.003	0.009	0.004	0.008	0.010	0.004	—0.001
Max.	r_s	—	—	0.579	0.747	—	-0.543	0.574	—	0.546
	p-value	—	—	0.009	<0.001	—	0.016	0.010	—	0.016
Mean	r_s	—	-0.540	0.541	0.569	—	—	—	—	—
	p-value	—	0.017	0.017	0.011	—	—	—	—	—
Organs at risk										
Brain stem max.	r_s	—	—	—	—	—	—	—	—	0.467
	p-value	—	—	—	—	—	—	—	—	0.038

(Continued)

Dose-volumetric parameter	$S_{0-0.4}$	$S_{0.4-0.8}$	$S_{0.8-1.2}$	$S_{1.2-1.6}$	$S_{1.6-2.0}$	Mean speed	A_{0-4}	A_{4-8}	A_{16-20}	Mean acceleration
Left parotid gland mean	r_s	-0.484	-	-	-	0.478	-	-	-	-
	p-value	0.031	-	-	-	0.033	-	-	-	-
Left optic nerve max.	r_s	-	-	-	-	-	-	-0.480	-	-
	p-value	-	-	-	-	-	-	-	0.032	-

$A_{1/n}$, the proportion of number of CPs of MLC accelerations ranging from / to $h\text{cm s}^{-2}$; CP, control point; $D_{n\%}$, dose received by $n\%$ of volume of structure; Max., maximum dose; Mean, mean dose; Min., minimum dose; r_s , Spearman's rho; $S_{1/n}$, the proportion of number of CPs with MLC speeds ranging from / to $h\text{cm s}^{-2}$.

Table 6. (Continued)

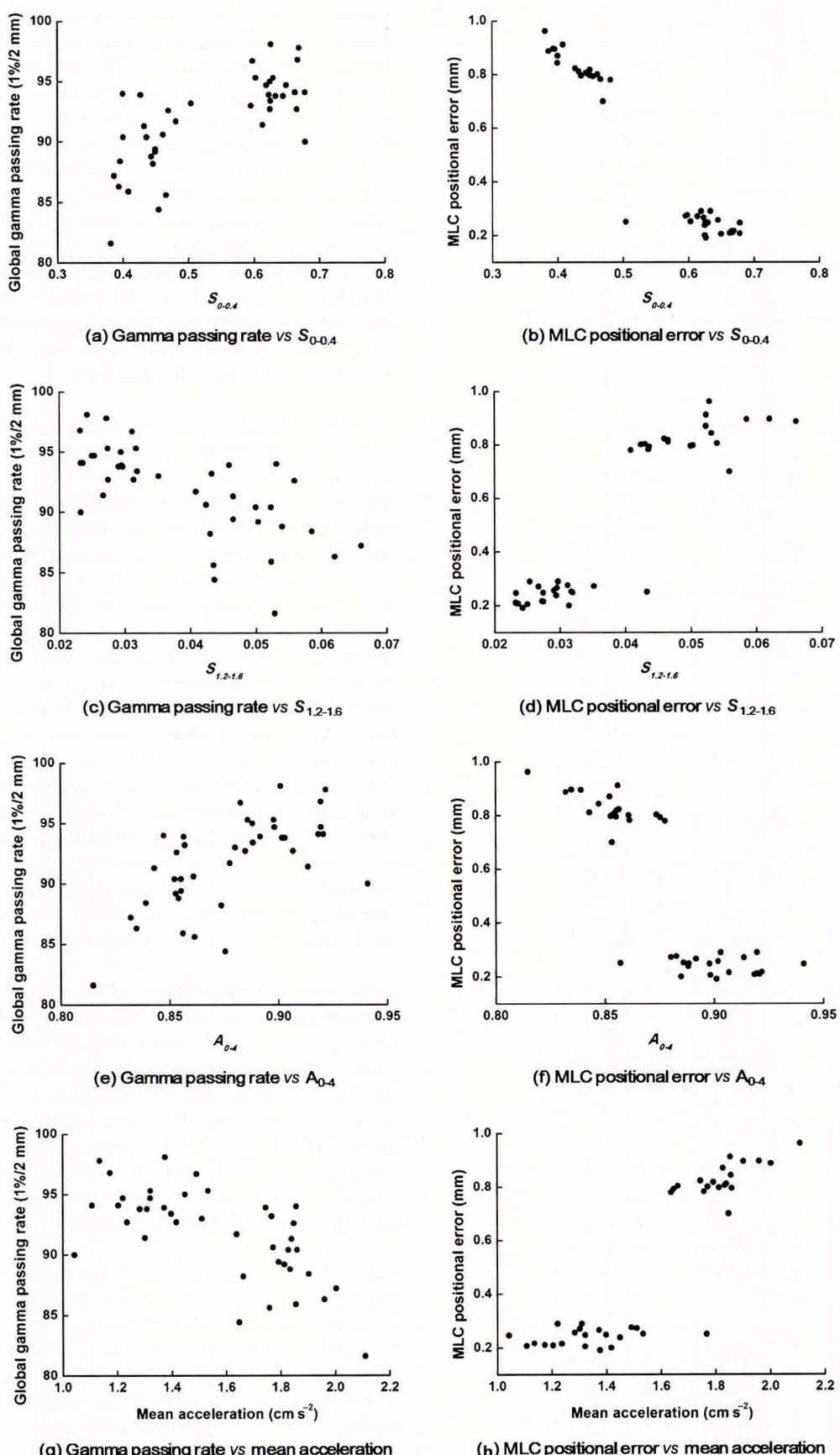
0.4 cm s⁻¹ or accelerations >4 cm s⁻² increased. When these proportions increased, both global and local gamma passing rates decreased, MLC positional errors increased and the magnitude of changes in dose–volumetric parameters increased, indicating a decrease in plan delivery accuracy. The global gamma passing rates with 1%/2 mm vs $S_{0-0.4}$ and A_{0-4} as well as MLC positional errors vs $S_{0-0.4}$ and A_{0-4} are plotted in Figure 3. This seems to be owing to the increased uncertainty in MLC movements by the increased MLC speeds and accelerations. Large uncertainties in MLC positions would cause the MLC positional errors and this might cause not only poor gamma passing rates but also large changes in dose–volumetric parameters between plan and delivery. Although poor gamma passing rates came from not only delivery errors but also TPS (eclipse) commissioning errors, the tendency of correlations of gamma passing rates to both MLC speeds and accelerations were similar with those of MLC positioning errors, which is irrelevant to the TPS commissioning errors.

Correlations of MLC speeds and MLC accelerations to the gantry angle errors showed the opposite tendency as that observed in gamma passing rates, MLC errors and changes in dose–volumetric parameters between plan and delivery. That is, gantry angle errors decreased as MLC speeds and accelerations increased. VMAT plans tend to be delivered with maximum gantry rotation speed if possible.^{26,33} If it is necessary to deliver large MUs at a specific sector of an arc, which cannot be delivered even with the maximum dose rate, the gantry rotation speed should be lowered.^{26,33} In that case, MLCs might not have to move fast compared with the case of the maximum rotation speed of gantry since more time would be given to MLCs to move for modulation of photon beams owing to slowing down of gantry rotation speed. Therefore, not all but some low MLC speeds and accelerations at certain CPs might indicate the changes in the gantry rotation speed, which could make more gantry angle errors. We guess that the opposite tendency of correlations where gantry angle errors decreased as MLC speeds and accelerations increased was owing to this reason. Further analysis on the relationship between MLC speeds and MLC accelerations with gantry angle errors will be performed as a future work.

In the case of the relationship of MU errors with MLC speeds and accelerations, no statistically significant correlations were observed. The average MU errors of the prostate and H&N VMAT plans in this study were only 0.160 ± 0.002 and 0.140 ± 0.130 , respectively, showing minimal differences between plan and delivery.²⁵ We guess that the reason for the lack of correlations between MU errors with MLC speeds and MLC accelerations was owing to the relatively accurate control system of MU delivery compared with the control systems of MLC movement or gantry rotation, as Nicolini et al²⁶ demonstrated.

Nelms et al¹⁵ previously showed that gamma passing rates had little clinical relevance by introducing intentional errors in intensity-modulated radiation therapy plans. In this study, the statistically significant r_s values ($p < 0.05$) between global gamma passing rates with 2%/2 mm gamma criterion, which has been recommended for VMAT pre-treatment QA in previous studies,^{7,8} and the dose–volumetric parameter changes were observed in 16 cases from a total of 35 tested cases (data are not

Figure 3. The global gamma passing rates with 1%/2 mm vs $S_{0-0.4}$ (a), $S_{1.2-1.6}$ (c), A_{0-4} (e) and mean accelerations (g) are plotted. The multileaf collimator (MLC) positional errors vs $S_{0-0.4}$ (b), $S_{1.2-1.6}$ (d), A_{0-4} (f) and mean accelerations (h) are also plotted.



shown). As shown in previous studies, gamma passing rates as well as analysis on the MLC speed and acceleration variations are indicators evaluating overall accuracy of VMAT delivery comprehensively.^{15,25} On the other hand, dose–volumetric parameter changes are indicators evaluating VMAT delivery accuracy partially for specific structures, since only part of the mechanical operation of the linac is involved in irradiation of a specific dose–volumetric parameter. For example, some, but not all, MLC movements were involved in the dose delivered to lens in the case of H&N VMAT plans. The mechanical or dosimetric errors involved in those 16 dose–volumetric parameters might lower the values of global gamma passing rates with the 2%/2 mm criterion. Therefore, global gamma passing rates with 2%/2 mm showed clinical relevance in 16 cases in this study. Since a detailed analysis on the relationship between gamma passing rates and changes in dose–volumetric parameters is out of the scope of this study, further analysis was not performed.

To comprehensively review the r_s values of MLC speeds and accelerations to the results of the three verification methods for VMAT delivery accuracy, $S_{1.2-1.6}$ and the mean values of MLC accelerations generally showed stronger correlations with statistical significances than did the others. The global gamma passing rates with 1%/2 mm vs $S_{1.2-1.6}$ and mean MLC acceleration as well as MLC positional errors vs $S_{1.2-1.6}$ and mean MLC acceleration are plotted in Figure 3. The highest performance was achieved with $S_{1.2-1.6}$ and mean MLC accelerations in the changes in dose–volumetric parameters, showing statistically significant r_s values in 14 and 12 cases, respectively. The $S_{1.2-1.6}$ and mean MLC acceleration also showed generally stronger correlations to plan delivery accuracy than did previously suggested indices, including MCS_v, LTMCS and MI_{SPORT}.²⁵ Since all VMAT plans in this study were clinically acceptable and the sample size was only 40, the potential and threshold values of $S_{1.2-1.6}$ and mean acceleration as modulation indices for VMAT remain unclear in lieu of further evidence. Therefore, further investigation should be carried out utilizing more VMAT plans, including clinically unacceptable plans owing to excessive modulation. Further investigation on $S_{1.2-1.6}$ and mean MLC acceleration will be performed as a future work.

Each of the mechanical parameters used for modulation of photon beam intensities of VMAT, which are MLC positions, gantry angles and dose rates, are synchronized with one another. In addition, the values of those mechanical parameters are determined at each CP considering mechanical limits and mutual operational synchronization when VMAT plans are optimized during the plan generation process. Therefore, by analysing the variations of MLC speeds and accelerations of VMAT plans, we could predict not only errors in

MLC positions but also gantry angle errors resulting in both poor gamma passing rates and differences in dose–volumetric parameters between plan and delivery. Although MLC speeds and accelerations varied within mechanical limits of the linac when generating VMAT plans, as the proportions of CPs with MLC speeds $>0.4 \text{ cm s}^{-1}$ and MLC accelerations $>4 \text{ cm s}^{-2}$ increased, differences between original treatment plans and actual delivery increased. If we control MLC movements at the planning stage to avoid creation of VMAT plans expected to be delivered inaccurately, and also limit the MLC speeds and accelerations in such a way as to not critically degrade plan quality, then we can increase our confidence that the plan will be delivered as intended. The results of this study seem to be used practically by limiting MLC speeds and accelerations to be <0.4 and 4 cm s^{-2} , respectively. Additionally, $S_{1.2-1.6}$ and mean MLC acceleration showed potential as modulation indices for VMAT, showing generally stronger correlations to VMAT delivery accuracy than to MCS_v, LTMCS and MI_{SPORT}.

The limitation of this study is that the investigated sections of MLC speeds as well as accelerations were divided randomly (intervals of 0.4 cm s^{-1} for speeds and 4 cm s^{-2} for accelerations). Therefore, although the results showed worse VMAT delivery accuracy as the portions of MLC speeds $>0.4 \text{ cm s}^{-1}$ and MLC accelerations $>4 \text{ cm s}^{-2}$ increased, those numbers, *i.e.* 0.4 and 4 cm s^{-2} , are not necessarily the optimal tolerance levels. To find optimal tolerance levels of both MLC speeds and accelerations for an accurate VMAT delivery, further investigation with fine resolution should be performed and this will be carried out as a future work. The other limitation of this study is that the data analysed in this study were acquired from a single TPS in a single institution. Moreover, we analysed only two kinds of VMAT plans, which were for H&N cancer and prostate cancer. To generalize the results, multicentre study with various TPS as well as various kinds of VMAT plans should be performed. This also will be carried out as a future work.

CONCLUSION

In this study, the variations in MLC speeds and accelerations at each CP were comprehensively analysed in relation to the plan delivery accuracy. Plan delivery accuracy was assessed using passing rates with the 2D gamma-index method, mechanical parameter differences between the original treatment plan and log files, and the changes in dose–volumetric parameters of plans reconstructed with log files. When MLC speed or MLC accelerations were >0.4 and 4 cm s^{-2} , respectively, the plan delivery accuracy decreased. Generally $S_{1.2-1.6}$ and mean acceleration of MLC showed stronger correlations to VMAT delivery accuracy than did other modulation indices, such as MCS_v, LTMCS and MI_{SPORT}.

REFERENCES

1. Yu M, Jang HS, Jeon DM, Cheon GS, Lee HC, Chung MJ, et al. Dosimetric evaluation of tomotherapy and four-box field conformal radiotherapy in locally advanced rectal cancer. *Radiat Oncol J* 2013; **31**: 252–9. doi: 10.3857/roj.2013.31.4.252
2. Otto K. Volumetric modulated arc therapy: IMRT in a single gantry arc. *Med Phys* 2008; **35**: 310–17.
3. Oh SA, Kang MK, Kim SK, Yea JW. Comparison of IMRT and VMAT techniques in spine stereotactic radiosurgery with international spine radiosurgery consortium consensus guidelines. *Prog Med Phys* 2013; **24**: 145–53.
4. Du W, Cho SH, Zhang X, Hoffman KE, Kudchadker RJ. Quantification of beam complexity in intensity-modulated radiation

- therapy treatment plans. *Med Phys* 2014; **41**: 021716. doi: 10.1118/1.4861821
- 5. Ezzell GA, Burmeister JW, Dogan N, LoSasso TJ, Mechalakos JG, Mihailidis D, et al. IMRT commissioning: multiple institution planning and dosimetry comparisons, a report from AAPM Task Group 119. *Med Phys* 2009; **36**: 5359–73.
 - 6. Ezzell GA, Galvin JM, Low D, Palta JR, Rosen I, Sharpe MB, et al; IMRT Subcommittee; AAPM Radiation Therapy Committee. Guidance document on delivery, treatment planning, and clinical implementation of IMRT: report of the IMRT Subcommittee of the AAPM Radiation Therapy Committee. *Med Phys* 2003; **30**: 2089–115.
 - 7. Fredh A, Scherman JB, Fog LS, Munck af Rosenschöld P. Patient QA systems for rotational radiation therapy: a comparative experimental study with intentional errors. *Med Phys* 2013; **40**: 031716. doi: 10.1118/1.4788645
 - 8. Heilemann G, Poppe B, Laub W. On the sensitivity of common gamma-index evaluation methods to MLC misalignments in Rapidarc quality assurance. *Med Phys* 2013; **40**: 031702. doi: 10.1118/1.4789580
 - 9. Kim JI, Park SY, Kim HJ, Kim JH, Ye SJ, Park JM. The sensitivity of gamma-index method to the positioning errors of high-definition MLC in patient-specific VMAT QA for SBRT. *Radiat Oncol* 2014; **9**: 167. doi: 10.1186/1748-717X-9-167
 - 10. Agnew CE, King RB, Hounsell AR, McGarry CK. Implementation of phantom-less IMRT delivery verification using Varian DynaLog files and R/V output. *Phys Med Biol* 2012; **57**: 6761–77. doi: 10.1088/0031-9155/57/21/6761
 - 11. Chandraraj V, Stathakis S, Manickam R, Esquivel C, Supe SS, Papanikolaou N. Consistency and reproducibility of the VMAT plan delivery using three independent validation methods. *J Appl Clin Med Phys* 2010; **12**: 3373.
 - 12. Manikandan A, Sarkar B, Holla R, Vivek TR, Sujatha N. Quality assurance of dynamic parameters in volumetric modulated arc therapy. *Br J Radiol* 2012; **85**: 1002–10. doi: 10.1259/bjr/19152959
 - 13. Schreibmann E, Dhabaan A, Elder E, Fox T. Patient-specific quality assurance method for VMAT treatment delivery. *Med Phys* 2009; **36**: 4530–5.
 - 14. Teke T, Bergman AM, Kwa W, Gill B, Duzenli C, Popescu IA. Monte Carlo based, patient-specific RapidArc QA using Linac log files. *Med Phys* 2010; **37**: 116–23.
 - 15. Nelms BE, Zhen H, Tomé WA. Per-beam, planar IMRT QA passing rates do not predict clinically relevant patient dose errors. *Med Phys* 2011; **38**: 1037–44.
 - 16. Giorgia N, Antonella F, Eugenio V, Alessandro C, Filippo A, Luca C. What is an acceptably smoothed fluence? Dosimetric and delivery considerations for dynamic sliding window IMRT. *Radiat Oncol* 2007; **2**: 42.
 - 17. Li R, Xing L. An adaptive planning strategy for station parameter optimized radiation therapy (SPORT): segmentally boosted VMAT. *Med Phys* 2013; **40**: 050701. doi: 10.1118/1.4802748
 - 18. Masi L, Doro R, Favuzza V, Cipressi S, Livi L. Impact of plan parameters on the dosimetric accuracy of volumetric modulated arc therapy. *Med Phys* 2013; **40**: 071718. doi: 10.1118/1.4810969
 - 19. McGarry CK, Chinneck CD, O'Toole MM, O'Sullivan JM, Prise KM, Hounsell AR. Assessing software upgrades, plan properties and patient geometry using intensity modulated radiation therapy (IMRT) complexity metrics. *Med Phys* 2011; **38**: 2027–34.
 - 20. McNiven AL, Sharpe MB, Purdie TG. A new metric for assessing IMRT modulation complexity and plan deliverability. *Med Phys* 2010; **37**: 505–15.
 - 21. Mohan R, Arnfield M, Tong S, Wu Q, Siebers J. The impact of fluctuations in intensity patterns on the number of monitor units and the quality and accuracy of intensity modulated radiotherapy. *Med Phys* 2000; **27**: 1226–37.
 - 22. Nauta M, Villarreal-Barajas JE, Tambasco M. Fractal analysis for assessing the level of modulation of IMRT fields. *Med Phys* 2011; **38**: 5385–93. doi: 10.1118/1.3633912
 - 23. Webb S. A simple method to control aspects of fluence modulation in IMRT planning. *Phys Med Biol* 2001; **46**: N187–95.
 - 24. Webb S. Use of a quantitative index of beam modulation to characterize dose conformativity: illustration by a comparison of full beamlet IMRT, few-segment IMRT (fsIMRT) and conformal unmodulated radiotherapy. *Phys Med Biol* 2003; **48**: 2051–62.
 - 25. Park JM, Park SY, Kim H, Kim JH, Carlson J, Ye SJ. Modulation indices for volumetric modulated arc therapy. *Phys Med Biol* 2014; **59**: 7315–40. doi: 10.1088/0031-9155/59/23/7315
 - 26. Nicolini G, Clivio A, Cozzi L, Fogliata A, Vanetti E. On the impact of dose rate variation upon RapidArc implementation of volumetric modulated arc therapy. *Med Phys* 2011; **38**: 264–71.
 - 27. Van Dyk J, Barnett RB, Cygler JE, Shragge PC. Commissioning and quality assurance of treatment planning computers. *Int J Radiat Oncol Biol Phys* 1993; **26**: 261–73.
 - 28. Almond PR, Biggs PJ, Coursey BM, Hanson WF, Huq MS, Nath R, et al. AAPM's TG-51 protocol for clinical reference dosimetry of high-energy photon and electron beams. *Med Phys* 1999; **26**: 1847–70.
 - 29. Poppe B, Blechschmidt A, Djouguela A, Kollhoff R, Rubach A, Willborn KC, et al. Two-dimensional ionization chamber arrays for IMRT plan verification. *Med Phys* 2006; **33**: 1005–15.
 - 30. Gloi AM, Buchana RE, Zuge CL, Goettler AM. RapidArc quality assurance through MapCHECK. *J Appl Clin Med Phys* 2011; **12**: 3251.
 - 31. Iftimia I, Cirino ET, Xiong L, Mower HW. Quality assurance methodology for Varian RapidArc treatment plans. *J Appl Clin Med Phys* 2010; **11**: 3164.
 - 32. Kerns JR, Childress N, Kry SF. A multi-institution evaluation of MLC log files and performance in IMRT delivery. *Radiat Oncol* 2014; **9**: 176. doi: 10.1186/1748-717X-9-176
 - 33. Vanetti E, Nicolini G, Nord J, Peltola J, Clivio A, Fogliata A. On the role of the optimization algorithm of RapidArc® volumetric modulated arc therapy on plan quality and efficiency. *Med Phys* 2011; **38**: 5844–56. doi: 10.1118/1.3641866

Copyright of British Journal of Radiology is the property of British Institute of Radiology and its content may not be copied or emailed to multiple sites or posted to a listserv without the copyright holder's express written permission. However, users may print, download, or email articles for individual use.